tributed throughout the bulk of the polymer film, such a mode might be observed in the Raman spectrum. At or near the PMDA–ODA surface, it might be observed in the HREELS impact scattering regime.

A previous HREELS study[4] of chromium deposition onto the PMDA–ODA surface has revealed the disappearance of the carbonyl peak with the appearance of an HREELS feature approximately 200 cm^{-1} below. It would be of interest to perform similar measurements at coverages significantly less than the chromium monolayer coverage reported.

Another feature of interest found upon complexing PMDA with a chromium atom is the overall enhancement of the FT-IR/HREELS intensities. This may not be straightforward to observe since it is generally not a simple matter to calibrate absolute experimental intensities. At any but the lowest concentrations of chromium, one expects the overall magnitude of the intensity to be attenuated upon successive chromium depositions. Perhaps such intensity enhancement as found in the present calculations can be observed at the lowest concentration regimes.

Acknowledgment. I am indebted to A. R. Rossi for making the HONDO 7 molecular orbital program available to me and for assistance with its execution.

Registry No. (PMDA)(ODA) (copolymer), 25038-81-7; (PMDA)(ODA) (SRU), 25036-53-7.

References and Notes

(1) DiNardo, N. J.; Demuth, J. E.; Clarke, T. C. *J. Chem. Phys.* **1986**, *85*, 6739.
(2) Pireaux, J. J.; Gregoire, C.; Thiry, P. A.; Caudano, R. *J. Vac. Sci. Technol.* **1987**, *A5*, 598.
(3) DiNardo, N. J.; Demuth, J. E.; Clarke, T. C. *J. Vac. Sci. Technol.* **1986**, *A4*, 1050.
(4) DiNardo, N. J.; Demuth, J. E.; Clarke, T. C. *Chem. Phys. Lett.* **1985**, *121*, 239.
(5) Pireaux, J. J.; Vermeersch, M.; Gregoire, C.; Thiry, P. A.; Caudano, R. *J. Chem. Phys.* **1988**, *88*, 3353.
(6) Hahn, P. O.; Rubloff, G. W.; Ho, P. S. *J. Vac. Sci. Technol.* **1984**, *A2*, 756.
(7) White, R. C.; Haight, R.; Silverman, B. D.; Ho, P. S. *Appl. Phys. Lett.* **1987**, *51*, 481.
(8) Ho, P. S.; Hahn, P. O.; Bartha, J. W.; Rubloff, G. W.; Legoues, F. K.; Silverman, B. D. *J. Vac. Sci. Technol.* **1985**, *A3*, 739.
(9) Atanasoska, L. J.; Anderson, S. G.; Meyer, H. M., III; Lin, Z.; Weaver, J. H. *J. Vac. Sci. Technol.* **1987**, *A5*, 3325.
(10) Silverman, B. D.; Sanda, P. N.; Ho, P. S.; Rossi, A. R. *J. Polym. Sci., Polym. Chem. Ed.* **1985**, *23*, 2857.
(11) Silverman, B. D.; Bartha, J. W.; Clabes, J. G.; Ho, P. S.; Rossi, A. R. *J. Polym. Sci., Polym. Chem. Ed.* **1986**, *24*, 3325.
(12) Silverman, B. D.; Sanda, P. N.; Clabes, J. G.; Ho, P. S.; Hofer, D. C.; Rossi, A. R. *J. Polym. Sci., Polym. Chem. Ed.* **1988**, *26*, 1199.
(13) Rossi, A. R.; Sanda, P. N.; Silverman, B. D.; Ho, P. S. *Organometallics* **1987**, *6*, 580.
(14) Ishida, H.; Wellinghoff, S. T.; Baer, E.; Koenig, J. L. *Macromolecules* **1980**, *13*, 826.
(15) Dupuis, M.; Watts, J. D.; Villar, H. O.; Hurst, G. J. B. HONDO Version 7, IBM Corporation, Scientific and Engineering Computations, Kingston, NY, 12401.
(16) Binkley, J. S.; Pople, J. A.; Hehre, W. J. *J. Am. Chem. Soc.* **1980**, *102*, 939.
(17) Takahashi, N.; Yoon, D. Y.; Parrish, W. *Macromolecules* **1984**, *17*, 2583.
(18) Dobbs, K. D.; Hehre, W. J. *J. Comp. Chem.* **1987**, *8*, 861.
(19) Graphics software from the Scientific and Engineering Computations Group, IBM Data Systems Division, Kingston, NY.
(20) Villar, H. O.; Dupuis, M.; Watts, J. D.; Hurst, G. J. B.; Clementi, E. *J. Chem. Phys.* **1988**, *88*, 1003.
(21) Amos, R. D.; Gaw, J. F.; Handy, N. C.; Carter, S. *J. Chem. Soc., Faraday Trans. 1* **1988**, *84*, 1247.
(22) Ibach, H.; Mills, D. L. *Electron Energy Loss Spectroscopy and Surface Vibrations*; Academic Press: New York, 1982.
(23) Thiry, P. A.; Liehr, M.; Pireaux, J. J.; Caudano, R. *Phys. Scr.* **1987**, *35*, 368.
(24) Johnson, C. K. ORTEP-II; A Fortran Thermal-Ellipsoid Plot Program For Crystal Structure Illustrations. Report ORNL-5138, 1976; Oak Ridge National Laboratory, Oak Ridge, TN.
(25) Burns, G. *Introduction to Group Theory with Applications*; Academic Press: New York, 1977; Appendix 7.

Crystal Structure of Poly(4-methyl-*m*-phenylene terephthalamide)

Kenji Okuyama,* Hiroyuki Hidaka, and Hironobu Ichige

Faculty of Technology, Tokyo University of Agriculture and Technology, Koganei, Tokyo 184, Japan

Masanori Osawa

Central Research Laboratory, Mitsui-Toatsu Chemicals, Inc., Kasama-cho, Totsuka-ku, Yokohama-shi, Kanagawa 247, Japan. *Received January 17, 1989; Revised Manuscript Received February 23, 1989*

ABSTRACT: The conformation and molecular packing of poly(4-methyl-*m*-phenylene terephthalamide) has been determined by X-ray diffraction. Unit cell dimensions were a = 8.57, b = 7.54, c (fiber axis) = 22.11 Å, $\alpha = \gamma = 90°$, and $\beta = 116.3°$. The space group symmetry was *I*1*a*1. A model with parallel 1/1 helices at the corner and center of the unit cell was refined simultaneously against X-ray intensity data and stereochemical restraints. Mainly because of the methyl moiety substituted to the *m*-phenylene, the torsion angles of the benzene rings measured from the amide planes were fairly deviated from the energetically stable angle. The polymer chains form a two-dimensional hydrogen-bonded network with bond lengths of about 2.8 Å, which makes the crystal structure very stable. The molecular cross-section and the packing coefficient of this polymer showed that the polymer chains were packed rather loosely compared with other wholly aromatic polyamides.

Introduction

Fibers made of poly(*p*-phenylene terephthalamide) and its isomer, poly(*m*-phenylene isophthalamide) (hereafter, abbreviated PPTA and MPIA, respectively), have been utilized in many fields because of their high thermal stability (decomposition temperature T_d = 500 and 415 °C, respectively). Poly(4-methyl-*m*-phenylene terephthalamide) (4M-MPTA), is a stereochemically intermediate compound of the above two aromatic polyamides with methyl substituent. In addition to the high thermal stability (T_d = 425 °C), 4M-MPTA shows good dimensional stability at high temperature, good morphological stability against flame, and good dyeing ability.[1] For example, fibers of 4M-MPTA shrink only by 18% of their original length at 480 °C. On the other hand, those of MPIA shrink by 61% and fuse together at the same temperature.

0024-9297/89/2222-3776$01.50/0

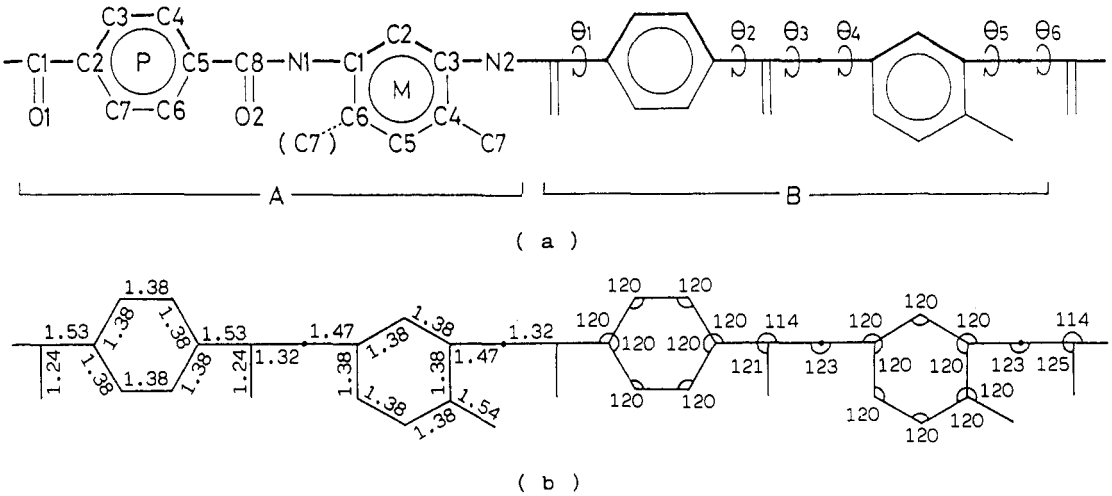

Figure 1. (a) Atomic numberings in a chemical unit of 4M-MPTA and dihedral angles varied in the refinement calculations. A fiber repeating unit consists of two chemical units, A and B. P and M denote *p*- and *m*-phenylene moieties, respectively. So far, there is no information on whether the methyl moiety (C7M) is located at C4M or C6M. The atoms linked by bold lines were treated as the main-chain atoms in the calculation, while the other atoms were treated as the pendant atoms.[3] (b) Bond lengths and bond angles used in the molecular model building and the refinement calculations. Both phenylene rings were treated as equilateral hexagons.

In order to gain an insight into the nature of these interesting properties, an X-ray structure analysis was carried out on poly(4-methyl-*m*-phenylene terephthalamide) fiber. We found from this analysis a quite different molecular conformation from those of other wholly aromatic polyamides and also found a strong hydrogen-bonded network.

Materials and Methods

(a) Materials. Poly(4-methyl-*m*-phenylene terephthalamide) was prepared by mixing terephthalic acid and 2,4-tolyl diisocyanate in an appropriate polar solvent at temperatures ranging from 100 to 250 °C. After polymerization was completed, the polymer solution was concentrated to 13 wt % by condensing under reduced pressure. The wet-spun fibers of 4M-MPTA were obtained by extruding the concentrated polymer solution from a capillary spinneret into an aqueous coagulation bath. The detailed procedure of the polymer synthesis, wet-spinning process, and fiber properties will be published elsewhere. After being drawn about 5 times at 375 °C in a few seconds, the polymer fiber was annealed at 360 °C for 30 min in order to improve the crystallinity of the specimen.

The density of the specimen was measured by a flotation method with a mixture of toluene and carbon tetrachloride.

(b) X-ray Diffraction. X-ray diffraction diagrams were recorded with a cylindrical camera using nickel-filtered Cu Kα radiation from a microfocus X-ray generator (ROTA FLEX RU-200, Rigaku Corp.). Coordinates of the Bragg reflections on the fiber diagram were measured in each quadrant using a STOE film-measuring device. Interplanar spacings were calculated from the coordinates for each spot, and the average values of the equivalent spots in the four quadrants were obtained. The unit cell dimensions were refined by a least-squares minimization. Fiber diagrams for intensity measurements were taken by the multiple film method. The intensities (I_o) were estimated by visual comparison with a standard intensity scale. These were corrected for the Lorentz and polarization factors (Lp) by using the following equation[2]

$$F_o = (I_o/Lp)^{1/2} \qquad 1/Lp = (\sin^2 2\theta - \zeta^2)^{1/2}/(1 + \cos^2 2\theta)$$

where F_o denotes the observed structure factor, θ denotes the Bragg angle of the reflection, and ζ denotes the axial coordinate in the reciprocal space. The absorption effect was not corrected in this study.

Since the number of independent observed reflections was only 19, the reflections below the observational threshold were also included in the data for the refinement calculations. That is, on each layer line, unobserved reflections with longer spacings than those of the observed ones were assumed to have one half of the observational threshold. These were used as intensity data only when the magnitude of the calculated structure amplitude became larger than that of the estimated structure amplitude ($|F_c| > |F_o|$) during the refinement calculations.

(c) Molecular Model Building. Molecular models having the appropriate helical symmetry and the fiber repeating period were generated using a linked-atom description with all bond lengths and angles held constant.[3] These values are shown in Figure 1, together with atomic numberings. As shown in the following section, the molecular structure of the 4M-MPTA was the 1/1 helix in which two chemical units (A and B in Figure 1a) were contained in the fiber repeating period, and the space group was determined to be $I121$ or $I1a1$. According to the space group, the molecular conformation was constrained by the corresponding crystal symmetry. In the case of $I1a1$, the polymer chain was required to have glide symmetry along the chain axis. For this requirement, the conformation angles in one chemical unit must have the same magnitude but opposite sign as the corresponding angle in the previous chemical unit. That is, $\theta_{1B} = -\theta_{1A}$, $\theta_{2B} = -\theta_{2A}$, $\theta_{3B} = -\theta_{3A}$, $\theta_{4B} = -\theta_{4A}$, $\theta_{5B} = -\theta_{5A}$, and $\theta_{6B} = -\theta_{6A}$. During the calculations, these were satisfied by applying the constraining conditions for the corresponding angles. On the other hand, in the case of $I121$, the 2-fold crystal axis must be located at the center of the *p*-phenylene ring, which requires the relationships $\theta_{1A} = \theta_{2A}$, $\theta_{3A} = \theta_{6B}$, $\theta_{4A} = \theta_{5B}$, $\theta_{5A} = \theta_{4B}$, $\theta_{6A} = \theta_{3B}$, and $\theta_{1B} = \theta_{2B}$. In both space groups, these restrictions from crystal symmetry left the six conformation angles as the explicit variables. The amide conformation angles, θ_3 and θ_6, were fixed to the trans in the early stage of the analysis. However, they were included in the refinement parameters at the final stage with restraining elastically to the trans conformation.

In order to make the starting model of the chain conformation, the four dihedral angles, (θ_{1A}, θ_{2A}, θ_{4A}, and θ_{5A} in the case of $I1a1$ or θ_{1A}, θ_{4A}, θ_{5A}, and θ_{1B} in the case of $I121$) were systematically changed. At first, the following assumptions were made to simplify the combinations of four dihedral angles. (1) These angles take only cis or trans conformation. (2) The methyl moiety attached to benzene can be ignored at the early stage of the analysis. The first assumption is borne out by the facts that the torsion angle between the amide plane and the benzene ring has been found at about ±30° in many compounds[4-9] including low molecular weight compounds. The second assumption was applied since there was no information about the location of the methyl moiety. That is, in the crystalline region of the 4M-MPTA, there was no evidence that the methyl moieties (C7M) are linked regularly to one site of the *m*-phenylene (C4M or C6M) or linked randomly. By these assumptions, a total of 16 ($=2^4$) models was deduced. In the following, the detailed procedure for the analyses will be mentioned only for the space group $I1a1$, since in addition to the fact that the procedure for $I121$ is very similar to that for $I1a1$, it was shown in the subsequent calculations that none of the

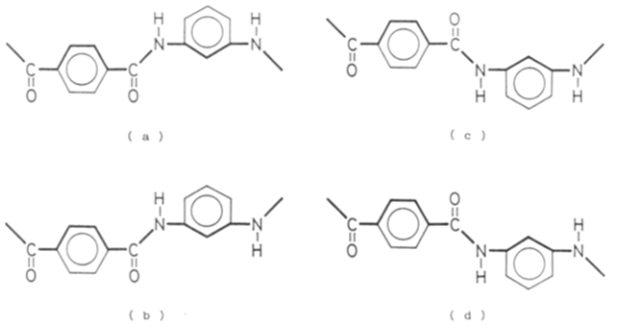

Figure 2. Four molecular models for the $I1a1$ space group. (a) $\theta_1 = \theta_2 = \theta_4 = \theta_5 = 0°$; (b) $\theta_1 = \theta_2 = \theta_4 = 0°$, $\theta_5 = 180°$; (c) $\theta_1 = 0°$, $\theta_2 = 180°$, $\theta_4 = \theta_5 = 0°$; (d) $\theta_1 = 0°$, $\theta_2 = 180°$, $\theta_4 = 0°$, $\theta_5 = 180°$.

packing models for $I121$ were plausible.

Among the 16 models for $I1a1$, half of them are independent, because the molecular models with $\theta_{1A} = \theta_{2A} = 0°$ or $\theta_{1A} = 0°$ and $\theta_{2A} = 180°$ are the same as those with $\theta_{1A} = \theta_{2A} = 180°$ or $\theta_{1A} = 180°$ and $\theta_{2A} = 0°$, respectively. Further, the models with $\theta_{1A} = \theta_{2A} = 0°$, $\theta_{4A} = 0°$, and $\theta_{5A} = 180°$ or $\theta_{1A} = 0°$, $\theta_{2A} = 180°$, $\theta_{4A} = 0°$, and $\theta_{5A} = 180°$ are the same as those with $\theta_{1A} = \theta_{2A} = 0°$, $\theta_{4A} = 180°$, and $\theta_{5A} = 0°$ or $\theta_{1A} = 0°$, $\theta_{2A} = 180°$, $\theta_{4A} = 180°$, and $\theta_{5A} = 0°$, since there is no unique direction along the polymer chain. In addition to the above reduction, there is another restriction to the molecular model. That is, because of the short contact between the carbonyl oxygen and the methyl moiety, the nearest dihedral angle θ_{4A} or θ_{5A} to the methyl moiety cannot take the trans conformation. Therefore, the models with $\theta_{4A} = \theta_{5A} = 180°$ are not plausible. The resultant four molecular models with cis or trans conformation for θ_{1A}, θ_{2A}, θ_{4A}, and θ_{5A} are shown in Figure 2.

At this stage, the first assumption was modified to a more reasonable one. That is, the four dihedral angles were assumed to be ±30° or ±150° instead of cis or trans conformation. Taking into account this modification and the glide symmetry along the chain axis, the independent number of combinations of four variables for the above models became $32(=4 \times 2^4/2)$. In the next section, the investigation was carried out for each of these 32 models.

(d) Packing Models and Their Refinement. Each molecular model was located at the corner (0, 0, 0) and at the body center ($^1/_2$, $^1/_2$, $^1/_2$) with the polymer chain parallel to the c axis of the crystal. For positioning the model in the unit cell, one additional parameter was used to define the relative axial orientation (μ). The glide symmetry in the molecular chain was forced to coincide with the crystallographic glide symmetry along the c axis by applying the constraining conditions about the relationships between the coordinates of the corresponding two atoms in the different repeating unit (A and B in Figure 1a). At each stage in the modeling and refinement of the structure, we sought to minimize the quantity Ω in the following least-squares fashion.

$$\Omega = \sum w_m(|_oF_m| - |_cF_m|)^2 + S\sum \epsilon_j + \sum \lambda_h G_h$$

The first summation in Ω ensures optimum agreement between the observed ($_oF_m$) and calculated ($_cF_m$) X-ray structure amplitudes. The second ensures the optimization of noncovalent interatomic interactions. The third imposes, by the method of Lagrange undetermined multipliers, the exact constraints we have chosen.

Atomic scattering factors for calculating structure factors were obtained using the method and values given in International Tables for X-ray Crystallography.[10] Computations were done on an ACOS 1000 computer at the Information Processing Center, Tokyo University of Agriculture and Technology.

Structure Determination

(a) Crystal Data. Figure 3 shows an X-ray fiber diagram from the 4M-MPTA specimen and its schematic illustration. The 19 observed independent reflections were indexed using a monoclinic unit cell with dimensions a = 8.57, b = 7.54, c (fiber axis) = 22.11 Å, $\alpha = \gamma = 90°$, and

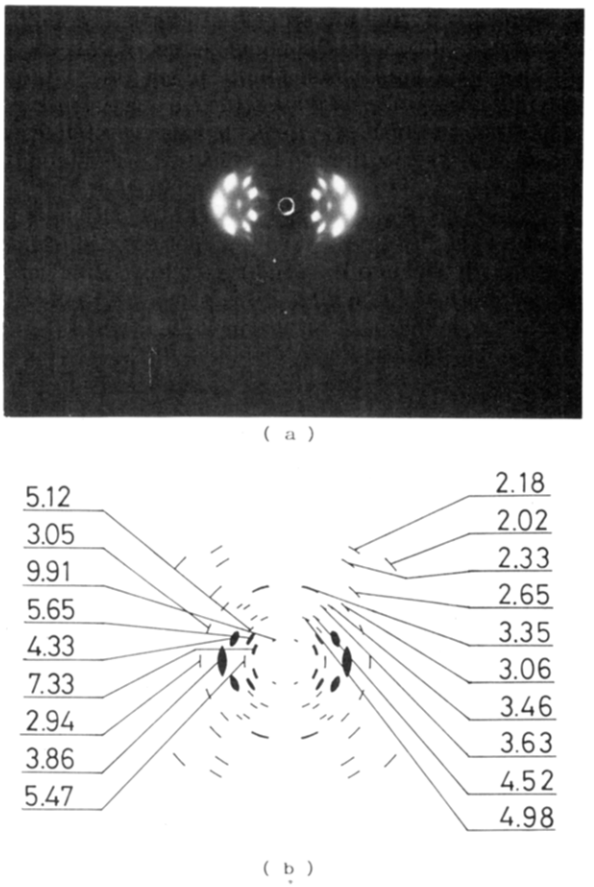

Figure 3. (a) X-ray diffraction pattern of 4M-MPTA taken by a cylindrical camera. (b) Its schematic illustration with measured spacings in angstroms.

$\beta = 116.3°$. Assuming that the unit cell contains four chemical repeating units, the calculated density (1.308 g/cm^3) agrees well with the observed value (1.30 g/cm^3). Since the extended length of a chemical repeating unit for the 4M-MPTA would be more than 12 Å, it is obvious that the polymer chain has more than one chemical repeating unit within a fiber repeating period of 22.1 Å. There are two ways to pack four chemical repeating units in the unit cell. In one case, the unit cell contains two chains and each chain has two chemical repeating units (two-chain model). In the other case, it contains only one chain with four chemical repeating units (one-chain model).

Measured and calculated spacings for observed reflections are listed in Table I. Since all observed reflections obeyed with the relation $h + k + l = 2n$ (n = integer), the following were the candidates for the space group of the 4M-MPTA crystal; $I121$, $I1m1$, $I1a1$, $I12/m1$, and $I12/a1$. Among these, the unit cell could accommodate four chemical repeating units of 4M-MPTA only when the space group is $I1a1$ or $I121$ and when the polymer chain has the corresponding crystallographic symmetry by itself. In both space groups, the one-chain model was not possible. That is, a unit cell contains two polymer chains with the 1/1 helical symmetry (or translational symmetry) parallel to the c axis. Each chain has two chemical repeating units in a fiber period of 22.1 Å. In the case of $I1a1$, the adjacent chemical units in the same molecule are related to each other by a glide symmetry running along the chain axis. In the case of $I121$, the 2-fold crystal symmetry axes are located at the center of the p-phenylene rings perpendicular to the ring planes. Since no plausible packing models were found for this space group after thorough analyses, the details of the analyses will be mentioned only for the space group $I1a1$.

Table I
Observed (d_o) and Calculated (d_c) Spacings Together with Observed (F_o) and Calculated (F_c) Structure Amplitudes for 4M-MPTA. Reflections in Parentheses Are Those below the Observational Threshold

do	d_c	h,k,l	F_o	F_c
equator				
5.32	5.38	1,1,0	69.58	46.01
3.65	3.84	2,0,0	243.82	250.94
	3.77	0,2,0		
2.66	2.69	2,2,0	49.45	67.32
1st layer				
7.23	7.05	0,1,1	151.30	127.04
2nd layer				
9.89	9.91	0,0,2	28.36	5.43
5.54	5.50	-1,1,2	138.30	151.69
4.16	4.28	-2,0,2	225.55	214.82
	4.21	1,1,2		
3rd layer				
5.02	4.97	0,1,3	66.01	82.88
	3.69	(-2,1,3)	22.99	27.49
	3.28	(-1,2,3)	24.75	32.89
2.81	2.80	1,2,3	47.44	64.95
	2.64	2,1,3		
4th layer				
4.94	4.96	0,0,4	40.51	27.05
4.44	4.39	-1,1,4	39.76	19.69
5th layer				
3.53	3.51	0,1,5	31.78	34.71
3.35	3.32	-2,1,5	33.13	45.33
2.89	2.86	-1,2,5	36.85	36.30
6th layer				
3.31	3.34	-2,0,6	110.54	77.42
	3.31	-1,1,6		
	3.30	0,0,6		
2.47	2.52	-3,1,6	62.90	70.23
	2.50	-2,2,6		
	2.49	1,1,6		
	2.48	0,2,6		
8th layer				
	2.70	(-2,0,8)	24.70	28.67
	2.57	(-1,1,8)	25.80	26.15
	2.48	(0,0,8)	26.71	7.73
2.20	2.27	-3,1,8	115.16	103.36
	2.19	-2,2,8		
	2.07	(0,2,8)	31.22	42.15
	2.02	(1,1,8)	31.83	27.02
	2.01	(-4,0,8)	32.03	7.08
	1.85	(-1,3,8)	34.29	25.23
1.76	1.77	-4,2,8	50.60	49.08
	1.76	2,0,8		
	1.73	-3,3,8		
9th layer				
	2.31	(-2,1,9)	27.41	47.71
	2.11	(0,1,9)	29.82	22.20
2.06	2.04	-1,2,9	53.46	49.58

The body-centered lattices for monoclinic unit cells are usually changed to the face-centered lattices. In the case of 4M-MPTA crystal, however, this was not done because of the very awkward unit cell dimensions (a = 19.86, b = 7.54, c (fiber axis) = 22.11 Å, and β = 23°) for the face-centered lattice.

(b) Molecular and Packing Structure. Figure 1 shows the atomic numberings for the chemical repeating unit of 4M-MPTA and the main-chain sequence (the bold line in Figure 1a), which was adopted in the linked-atom calculations. Among the 32 molecular models, two models, in which the starting dihedral angles θ_1, θ_2, θ_4, and θ_5 are 30°, -150°, -30°, and -30° and (30°, 150°, -30°, and -30°, respectively, ended up in almost the same conformation (-89°, -66°, -87°, and -64°) after several refinement cycles. This conformation was found to be suitable in terms of interatomic short contacts, hydrogen bond formations, and agreement between obserrved and calculated structure amplitudes (R = 0.36). The rest of the models were not possible mainly because of short atomic interactions between adjacent molecules. Therefore, the above structure alone was further refined and the discrepancy factor (R) was reduced to 0.27. At this tage, the methyl moieties were linked to the C4M and/or C6M atom of the m-phenylene, and each structure was refined another several cycles including the amide dihedral angles, θ_3 and θ_6, in the refinement parameters. An overall isotropic temperature factor (that is, attenuation factor B in LALS) was fixed to 10.0 in order to reduce the number of parameters, since the value B did not vary significantly even when this was included in the refinement parameters. The resultant structures are summarized in Table II.

Table II
Final Values of Refinement Parameters for Three Molecular Models of 4M-MPTA[a]

	model A	model B	model C
C7M linkage	C4M	C6M	C4M and C6M with half occupancies
dihedral angles, deg			
θ_{1A}	-109.0	-93.0	-112.0
θ_{2A}	-78.0	-60.9	-67.7
θ_{3A}	178.0	-179.8	178.0
θ_{4A}	-58.0	-80.6	-62.9
θ_{5A}	-73.2	-60.7	-71.4
θ_{6A}	-173.7	-177.4	-174.1
Eulerian angles, deg			
ϵ_x	101.5	101.7	101.6
ϵ_y	56.5	56.4	56.1
ϵ_z	-34.6	-34.0	-32.7
scale factor	0.5212	0.5029	0.4853
s	1.984	1.942	1.933
μ	67.2	68.4	69.6
R	0.21 (0.23)	0.16 (0.18)	0.17 (0.21)
R_w	0.21 (0.23)	0.15 (0.16)	0.18 (0.20)
H bond length, Å	2.68	2.74	2.65
	2.78	2.90	2.81

[a] Eulerian angles, ϵ_x, ϵ_y, and ϵ_z, relate the chain orientation to the lattice coordinates. s and μ denote the cylindrical radius of the origin atom in the molecular coordinates and the axial orientation angle of the molecule, respectively. Dihedral angles in the B chemical repeating unit are obtained by the relation of $\theta_{nB} = -\theta_{nA}$. R factors for the reflections including unobserved ones are in parentheses. Attenuation factor B was fixed to 10.0 during the refinement calculations.

Table III
Fractional Atomic Coordinates of 4M-MPTA

atom	x	y	z	atom	x	y	z
O1P	-0.158	0.168	0.482	N1M	0.019	0.521	0.225
C1P	-0.023	0.128	0.477	C1M	0.034	0.610	0.169
C2P	0.024	0.216	0.425	C2M	0.056	0.511	0.120
C3P	-0.038	0.147	0.361	C3M	0.070	0.595	0.067
C4P	0.004	0.226	0.314	C4M	0.063	0.777	0.063
C5P	0.108	0.375	0.331	C5M	0.042	0.876	0.111
C6P	0.171	0.444	0.395	C6M	0.027	0.793	0.164
C7P	0.129	0.365	0.442	C7M	0.003	0.903	0.218
C8P	0.155	0.463	0.279	N2M	0.093	0.489	0.016
O2P	0.308	0.475	0.288				

On the other hand, in the case of the $I121$ space group, none of the 32 molecular models emerged as a reasonable structure after similar refinement procedures as those done for $I1a1$. These structures had fairly high discrepancy factors, fatal short contacts between adjacent molecules, and no hydrogen bond formation.

The atomic coordinates of the molecular model with the methyl moiety linked to the C6M atom (model B in Table II) are listed in Table III. The packing structures are shown in Figures 4 and 5.

Results and Discussion

(a) Three Packing Models. Since there is no information about preferential reactivities of 2,4-tolyldiisocyanate with terephthalic acid, three molecular models

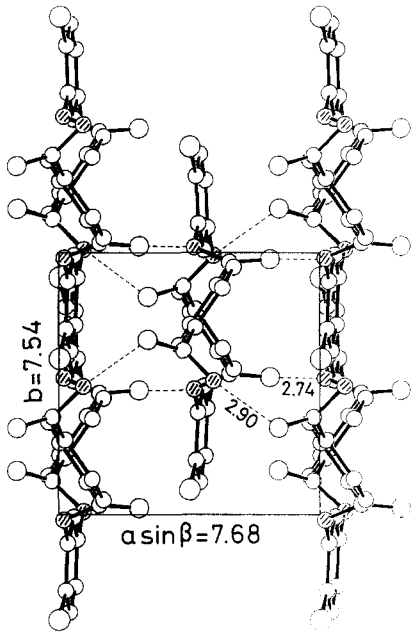

Figure 4. Packings of the 4M-MPTA chains in the unit cell (ORTEP[13] drawing). Projection parallel to the *c* axis. Hydrogen bonds are shown by broken lines.

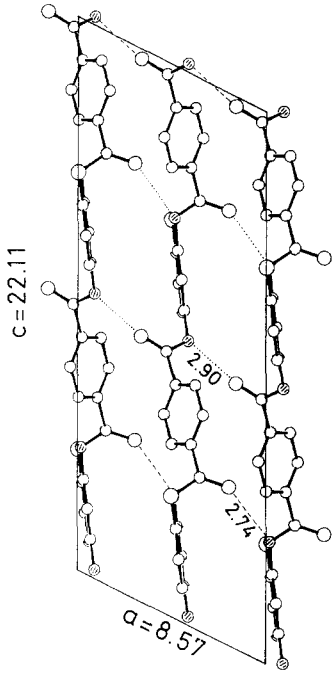

Figure 5. Crystal structures of 4M-MPTA projected along the *b* axis. Two corner chains and one body-centered chain are shown.

with the methyl moiety located at different positions were considered. That is, if there is a considerable reactivity difference between isocyanates at 2- and 4-positions, the methyl moieties will be located regularly on the C4M or C6M atom after the polymerization. These correspond to models A and B, respectively. On the other hand, if there is no reactivity difference, *m*-phenylene with methyl moieties linked to the C4M or C6M will be randomly distributed in the polymer chain, which corresponds to model C. Final refinement parameters for these three models are listed in Table II. Even though these models have almost the same conformation to each other, model B shows better agreement between observed and calculated structure amplitudes (R_w = 0.15) compared with those of other models (R_w = 0.21 for A and 0.18 for C). The molecular conformations in models A and C deviate slightly from that of model B to avoid the short contacts between the methyl moiety linked to the C4M and its surroundings. Taking into account the number of reflections and the crystallinity of the specimen, however, it is better not to conclude that the model B structure is dominant in the whole crystalline region of the 4M-MPTA. The crystalline region presumably consists of a mixture of these three models.

(b) Molecular Structure. The planarity of the amide bonds is fairly good, especially in model B (θ_3 and θ_6 in Table II). However, the values of other dihedral angles, θ_1, θ_2, θ_4, and θ_5, were very different from those expected from the related compounds.[4-9] Structure analyses for the wholly aromatic polyamides, such as PPTA,[5] MPIA,[6] and polybenzamide[4] (abbreviated as PBA hereafter), revealed that the torsion angles of the benzene rings measured from the amide planes were about 30°, which was also borne out as the most stable by conformational energy calculations.[11] In the case of 4M-MPTA, these angles are fairly deviated from the energetically stable angle (Table II). The reason for the deviations of θ_4 and θ_5 is attributable to the methyl moiety linked to the C4M or C6M atom. That is, to avoid the severe intramolecular contacts between the methyl moiety and the amide plane, it is necessary for these angles to be about ±90°. Futher, in the case of models A and C, the intermolecular short contacts between the methyl moiety and the *p*-phenylene ring force the dihedral angles of θ_1 and θ_2 to be about ±90°. In model B, these angles are also restricted to be about ±90° because of the short contacts between the carbonyl segment and the *p*-phenylene ring in the adjacent molecule.

(c) Hydrogen Bond. Two hydrogen bond donors in the chemical repeating unit are both participating in hydrogen bonds with carbonyl oxygens in neighboring molecules along the *a* direction (Figure 4). In comparison to the rather long hydrogen bonds in other aromatic polyamides (3.01 Å in PBA, 3.04 Å in PPTA, and 3.18 Å in MPIA), those of 4M-MPTA have ideal lengths (2.7 ~ 2.9 Å) as a NH···O=C type hydrogen bond (Table II). Further, differently from the one-dimensional hydrogen bonds in the crystals of PPTA and PBA, the 4M-MPTA crystal shows two-dimensional hydrogen-bond networks similar to those in MPIA. This two-dimensional network with rather strong hydrogen bonds makes the crystal structure of 4M-MPTA very stable, which is presumably one of the main reasons for the high dimensional stability of this polymer at elevated temperature.

(d) Packing Density. Wholly aromatic polyamides consisting of para-substituted phenylene, such as PBA and PPTA, have small molecular cross-sections (about 20 Å^2) compared with other types of polymer chains. Since their cross-sections were comparable to that of the simplest polymer, polyethylene, these polymer chains must be packed in very compact fashion. On the other hand, the aromatic polyamide with meta-substituted phenylene (MPIA) has a somewhat larger cross-section (24 Å^2). Contrary to the expectation from the intermediate linkage between the above para- and meta-substituted polyamide molecules, the 4M-MPTA crystal shows a rather large cross-section (29 Å^2). This fact indicates that the methyl moiety linked to the *m*-phenylene significantly affects the molecular packing and makes it very loose. Consequently, the packing density of 4M-MPTA (1.30 g/cm^3) is considerably low compared with those of other aromatic polyamides (PBA, 1.49 g/cm^3; PPTA, 1.44 g/cm^3; MPIA, 1.38 g/cm^3). The difference in packing states between the 4M-MPTA and other aromatic polyamides is also remarkable in terms of the packing coefficient (*K*) proposed

by Kitaigorodskii.[12] The value of K for the 4M-MPTA (0.71) falls into the average value (0.681) of 70 polymer compounds investigated in ref 12. However, the coefficients of other aromatic polyamides (PBA, 0.82; PPTA, 0.80; MPIA, 0.77) deviate significantly from the mean value, which shows that these polymers have highly ordered forms and pack very compactly. The looseness of packing in the solid state of 4M-MPTA is closely related to the good dyeing ability of this polymer compared with other aromatic polyamides.

Registry No. 4M-MPTA (SRU), 59113-46-1; 4M-MPTA (copolymer), 84892-96-6.

References and Notes

(1) Morishita, N. *Nikko Materiaru* **1986**, *4*, 14–17.
(2) Cochran, W. *J. Sci. Instrum.* **1948**, *25*, 253–255.
(3) Smith, P. J. C.; Arnott, S. *Acta Crystallogr.* **1978**, *A34*, 3–11.
(4) Okuyama, K.; Arikawa, H.; Chen, M.; Takayanagi, M.; Chatani, Y.; Hasegawa, R.; Tadokoro, H. *Sen'i Gakkaishi* **1989**, *45*, 141–146.
(5) Northolt, M. G. *Eur. Polym. J.* **1974**, *10*, 799–804.
(6) Kakida, H.; Chatani, Y.; Tadokoro, H. *J. Polym. Sci., Polym. Phys. Ed.* **1976**, *14*, 427–435.
(7) Yasuoka, N.; Kasai, N.; Kakudo, M. *Bull. Chem. Soc. Jpn.* **1969**, *42*, 91–101.
(8) Pineault, C.; Brisse, F. *Acta Crystallogr.* **1983**, *C39*, 1434–1437.
(9) Orii, S.; Nakamura, T.; Takai, Y.; Sasada, Y.; Kakudo, M. *Bull. Chem. Soc. Jpn.* **1963**, *36*, 788–793.
(10) *International Tables for X-ray Crystallography*; Ibers, J. A., Hamilton, W. C., Eds.; Kynoch Press: Birmingham, England, 1974; Vol. 4, pp 71–147.
(11) Tashiro, K.; Kobayashi, M.; Tadokoro, H. *Macromolecules* **1977**, *10*, 413–420.
(12) Slonimskii, G. L.; Askadskii, A. A.; Kitaigorodskii, A. I. *Vysokomol. Soedin.* **1970**, *A12*, 494–512.
(13) Johnson, C. K. Report ORNL-5138, 1976; Oak Ridge National Laboratory: Oak Ridge, TN.

Use of Moment Analysis in Inverse Gas Chromatography

Jing-Yu Wang and Gérard Charlet*

Department of Chemistry and Centre de Recherches en Sciences et Ingénierie des Macromolécules (CERSIM), Université Laval, Cité Universitaire, Quebec, Canada G1K 7P4.

Received October 26, 1988; Revised Manuscript Received February 9, 1989

ABSTRACT: The use of the statistical moments of the outlet concentration profile in inverse gas chromatography is critically examined. With the help of a data acquisition procedure that limits the incidence of noise on the chromatogram and a chromatographic assembly where most extra column contributions to dead volume are suppressed, a viable moment analysis of the elution profiles can be performed. The first moment provides the proper measure of retention, reproducible and independent of flow rate. Measurements carried out on polystyrene deposited in a packed column show that the drop in the retention diagram, usually observed at the glass transition temperature, T_g, when retention volumes are calculated from the position of the peak maximum, is not an indication of the onset of a different retention mechanism but rather an artifact of the use of an inappropriate retention parameter. Calculations of the activity coefficient of chloroform at infinite dilution in polystyrene further demonstrate the importance of using the first moment of the elution profile instead of its maximum, even at temperatures much higher than T_g.

Introduction

During the last 20 years, inverse gas chromatography (IGC) has become a widely used method for the physicochemical characterization of polymeric materials.[1-12] materials.[1-12] It is an invaluable tool for the study of the polymer structure: melting or glass transitions are largely reflected in the retention of a volatile solute because of the changes they induce, respectively, in the solubility and the rate of diffusion of the low molecular weight probe in the polymer. The sensitivity of the retention behavior on the structure of the stationary phase has prompted a large variety of investigations by IGC, for instance, studies of the kinetics of polycondensation[13] or the morphology of inorganic material–polymer composites.[14] Thermodynamic studies of polymer–solvent interactions also constitute a large part of IGC measurements. The weight fraction activity coefficient, the Flory–Huggins interaction parameter, and the partial molar enthalpy of mixing of the volatile probe at infinite dilution in the polymer can be derived from retention data, provided equilibrium conditions are achieved between the mobile and the stationary phases. The method has been extended to mixed stationary phases, allowing for measurement of the interaction between the two components of a polymer blend and the study of their miscibility. In addition to equilibrium parameters, dynamic properties can be studied by IGC. The diffusion coefficients of volatile liquids in the bulk polymer, again at infinite dilution of probe, can be estimated from the effect of the polymer resistance to mass transfer on the shape of the chromatographic peak.[15-18] The knowledge of diffusion coefficients has a large industrial importance, e.g., in the production of thermoplastic foams or the removal of residual monomer and solvent after polymerization.[19]

The experimental procedure of IGC recently underwent a critical evaluation by Munk et al.[9-11,17] Such aspects as the role of inert support[10] or the effect of the amount of probe injected[11] have been investigated, improving the reliability of the IGC method. However, one facet still needs clarification in the case of thermodynamic studies, namely the effect of ignoring the asymmetry of the elution curve. The primary datum gathered by IGC is V_N, the net retention volume, which represents the volume of carrier gas required to elute the probe. It is calculated from the average flow rate in the column and the net retention time of the solute, i.e., the difference between the first statistical moments of the elution curves of the solute and a marker gas.[8] With a few exceptions,[16,20] the difference between the peak maxima is quite generally used in the literature, thereby assuming peak symmetry. This assumption is notoriously invalid for polymers at temperatures close to their glass transition.[6] In this range, the difference between V_N and V_N^{max}, the net retention volume calculated from the peak maxima, is of no consequence for qualitative

0024-9297/89/2222-3781$01.50/0